Environ Earth Sci
DOI 10.1007/s12665-014-3253-2

THEMATIC ISSUE

# Assessing the saltwater remediation potential of a three-dimensional, heterogeneous, coastal aquifer system

## Model verification, application and visualization for transient density-driven seawater intrusion

**Marc Walther · Lars Bilke · Jens-Olaf Delfs · Thomas Graf · Jens Grundmann · Olaf Kolditz · Rudolf Liedl**

Received: 22 October 2013 / Accepted: 31 March 2014


**Abstract** This paper evaluates the remediation potential of a salinized coastal aquifer by utilizing a scenario simulation. Therefore, the numerical model OpenGeoSys is first validated against analytical and experimental data to represent transient groundwater level development and variable density saline intrusion. Afterwards, a regional scale model with a three-dimensional, heterogeneous hydrogeology is calibrated for a transient state and used to simulate a best-case scenario. Water balances are evaluated in both the transient calibration and scenario run. Visualization techniques help to assess the complex model output providing valuable insight in the occurring density-driven flow processes. Furthermore, modeling and visualization results give information on the time scale for remediation activities and, due to limitations in data quality and quantity reveal potential for model improvement.

**Keywords** Groundwater modeling · Density-dependent · Saltwater intrusion · OpenGeoSys · Model validation benchmark · Transient calibration · Scenario simulation · Remediation potential · Visualization

**Electronic supplementary material** The online version of this article (doi:10.1007/s12665-014-3253-2) contains supplementary material, which is available to authorized users.

M. Walther · R. Liedl
Institute for Groundwater Management, Technische Universität Dresden, Dresden, Germany

M. Walther (✉) · L. Bilke
Department of Environmental Informatics, Helmholtz-Centre for Environmental Research, Leipzig, Germany
e-mail: marc.walther@ufz.de

L. Bilke
e-mail: lars.bilke@ufz.de

J.-O. Delfs
Institute of Geosciences, Christian-Albrechts-Universität zu Kiel, Kiel, Germany

T. Graf
Institute of Fluid Mechanics and Environmental Physics in Civil Engineering, Leibniz Universität Hannover, Hannover, Germany

J. Grundmann
Institute of Hydrology and Meteorology, Technische Universität Dresden, Dresden, Germany

O. Kolditz
Applied Environmental Systems Analysis, Technische Universität Dresden, Dresden, Germany

## Introduction—motivation and background

In regions with limited surface water availability, groundwater resources are often intensively used for various applications. Pumping activities that satisfy irrigational demands account for ca. 70 % of the world's freshwater usage and often result in enormous groundwater table drawdown (Siebert et al. 2010). With the natural balance of fresh and saline water being disturbed, marine saltwater intrudes further into coastal aquifers. As saline water cannot be used for irrigation, long-term stability of the aquifers is a common goal for water management in (semi-) arid regions (Krueger and Teutsch 2013).

Numerical models offer the capability to evaluate possible management strategies of real-world applications (e.g., Narayan et al. 2007; Giambastiani and Antonellini 2007; Abd-Elhamid and Javadi 2011; Werner et al. 2012). In this study, we use numerical simulations to assess the development of the groundwater levels and saline intrusion in the past and project a future scenario. This paper extends the work of Walther et al. (2012) and (2013), who already

Published online: 22 April 2014

calibrated a pre-development steady state and presented a workflow to illustrate complex model output.

The study area is located in the southern Al-Batinah region at the northern coast of Oman, including the near coastal regions of the wadis Ma'awil and Bani Kharus. Highly productive soils, formed from silty fluviatile sediments, have sustained a large amount of agriculture for hundreds of years [Bureau de Recherches Géologiques et Minières (BRGM) 1992]. The local aquifers that are used for abstraction of groundwater mainly consist of layered marine, aeolian, and fluviatile deposits with strong heterogeneity arising from its development. Source for irrigation was groundwater from hand-dug wells until the 1970s. From then, extensive construction of borehole wells increased abstraction rates tremendously, lowering the water table and, thus, promoting saline intrusion. While different approaches tackle various challenges on the surface water side to provide long-term stable, profitable water availability (Kalbus et al. 2011; Schütze et al. 2012; Grundmann et al. 2012), this paper will focus on the assessment of the subsurface groundwater resources.

Numerical tools need to reproduce the relevant processes of the investigated system sufficiently well (Kolditz et al. 2012b). Therefore, we firstly validate the numerical model against laboratory data for transient conditions. Afterwards, a calibration and scenario simulation are presented to evaluate future remediation potential of the salinized parts of the aquifer. Results are visualized in various ways to properly interpret the complex model output.

## Methods and concepts

### Numerical simulation tool

To simulate groundwater flow and mass transport, the numerical modeling tool OpenGeoSys was utilized (OGS, Kolditz et al. 2012a). OGS was used before for several density-driven flow applications (Kalbacher et al. 2011; Park and Aral 2008). Governing equations follow common standards for groundwater flow and mass transport in porous media and are given in Walther et al. (2012). OGS employs an approach from Sugio and Desai (1987) to simulate an unconfined groundwater table. Equation of state for density is a linear relationship which is reported to be sufficient for marine water density (Park 2004). The numerical model is based on the Galerkin-FEM method. The validity of level 1 Oberbeck–Boussinesq approximations for the variable density flow and transport process was shown in Kolditz et al. (1998).

### Visualization tool

Modeling results are visualized using ParaView (PV, Henderson 2007), a data analysis and visualization application based on the Visualization Toolkit (VTK, Schroeder et al. 2006). VTK employs a filter pipeline model that enables the user to combine a wide variety of visualization algorithms including contouring, glyphing, thresholding, slicing, or streamlining.

PV offers a client–server architecture to handle large datasets. The server processes the data and generates the visualization on a powerful computer cluster. Results of today's increasingly detailed or regional to larger scale setups often are tremendous data sets, which exceed bandwidth limitations to transfer output data from simulation clusters to local personal computers. Since the computational burden grows according to the detail in modeling and visualization, more and more visualization tools must run directly on the cluster and only transmit pre-rendered, lower sized data packages. Then, only the resulting images are sent to the user client. Data sets of simulation output are $\approx$ 150 MB per time step resulting in a total of $\approx$ 75 GB for the long-term scenario simulation. Processed and transmitted visualization data from the server are less than 2 MB per figure.

### Model verification

Before applying OGS in a regional scale model, we used two benchmarks to ensure correct representation of the relevant processes. First, we used the analytical Theis solution (Theis 1935) to validate the transient groundwater drawdown due to pumping activity. For a small drawdown in relation to the aquifer thickness, this method is applicable even for unconfined conditions, while for a larger drawdown, an adapted approach should be used (see Neuman 1974).

Numerical results of the first benchmark are in very good agreement with the analytical solution. Small deviations occur in direct vicinity of the pump or after long simulation times, when the assumption of an infinitely large aquifer cannot hold any more and the drawdown due to pumping has significant influence on the outer boundary condition. For reasons of space limitation, we do not show the results of the first benchmark here, but focus on a second one that features transient, density-dependent saltwater intrusion (see Sect. "Transient Goswami-Clement Benchmark").

### Remediation potential

To visualize the capability of the regional scale aquifer system to return to a near-natural state, we define the remediation potential $\Phi$ of the upper aquifer from salinity half-life after pump stop in the scenario simulation as

$$\Phi = 1 - c_{\mathrm{rel}} \cdot \frac{\lambda}{\lambda_{\max}} \quad (1)$$

where $c_{\mathrm{rel}}$ is relative concentration of salinity 10 m below groundwater level in 2005, $\lambda$ is half-life of $c_{\mathrm{rel}}$. and $\lambda_{\max}$ is

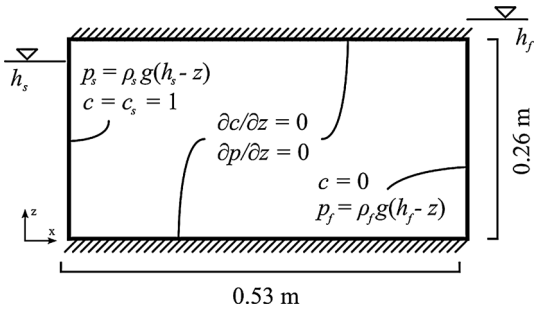


**Fig. 1** Model domain and boundary conditions after Goswami and Clement (2007) (altered, not to scale)

**Table 1** Benchmark parameters for Goswami–Clement problem

| Parameter | Value |
|---|---|
| Freshwater head $h_f$ (m) | 0.267 |
| Saltwater head $h_s$ (m) | 0.255 |
| Porosity $\varphi$ (−) | 0.385 |
| Permeability $\kappa$ ($m^2$) | $1.239 \times 10^{-9}$ |
| Dynamic viscosity $\mu$ (Pa s) | $1 \times 10^{-3}$ |
| Freshwater density $\rho_f$ (kg $m^{-3}$) | 1,000 |
| Saltwater density $\rho_s$ (kg $m^{-3}$) | 1,026 |
| Longit./transv. dispersivity $\alpha_{l/t}$ (m) | $1 \times 10^{-3}/1 \times 10^{-4}$ |
| Diffusion coefficient $D_m$ ($m^2$ $s^{-1}$) | 0 |
| Residual reduction factor $\zeta_{res}$ (−) | $1 \times 10^{-4}$ |
| Residual reduction pressure $p_{res}$ (Pa) | 100 |

maximum of $\lambda$. Comparable to the well known half-life of a decaying element, the salinity half-life $\lambda$ describes the time until the concentration of a mesh node reaches half of its value in the year 2005. The qualitative value $\Phi$ had to be multiplied with $c_{rel}$ to avoid overestimations for cells with initially already low salinity. The parameter has a range of $0 < \Phi < 1$, with $\Phi = 0$ as the lowest and $\Phi = 1$ as the highest potential for remediation.

## Transient Goswami–Clement benchmark

### Problem description

In the following, we present a benchmark to verify the capabilities of OGS to model transient, variable density groundwater flow, and transport. In Goswami and Clement (2007), a saltwater intrusion experiment similar to Henry (1960) using a laboratory scale tank is shown (hereafter referred to as the Goswami–Clement problem). OGS model results are compared against data from laboratory experiments and numerical SEAWAT simulations (Langevin and Guo 2006). This benchmark is an extension to the steady-state case documented in Walther et al. (2012).

### *Methods and model setup*

The Goswami–Clement problem features a horizontally intruding and withdrawing saltwater front in an initially present freshwater environment. The conceptual model is depicted in Fig. 1, important model parameters are listed in Table 1. For comparability reasons, the model setup and parameterization was followed as described by Goswami and Clement (2007).

The saltwater reservoir is situated on the left side of the tank, a freshwater reservoir on the right side. General flow points from right to left in the nearly homogeneous, isotropic material. Dimensions of the experimental tank were $0.53 \times 0.26 \times 0.027\,m^3$ (length × height × width). A vertical $x-z$ model domain was constructed using a grid resolution of uniform, rectangular quad-elements each $\Delta x = \Delta z = 5 \times 10^{-3}$m in size. At top and bottom edges, boundary conditions are 2nd-type NO-FLOW for flow and transport. Applied to the vertical edges are 1st-type boundary conditions as linear pressure gradients $p_i(z) = \rho_i g(h_i - z)$ for groundwater flow including the respective fluid densities $\rho_{f/s}$ as well as pressure heads $h_{f/s}$ of fresh or saltwater, respectively. Transient states TS1 (transition of steady-states SS1 to SS2) and TS2 (SS2 to SS3) for experiments and simulations are controlled by an instantaneous variation of the right-side freshwater pressure head. Constant concentration 1st-type boundary conditions are $c = 0$ and $c = c_s = 1$ on the fresh and saltwater side, respectively.

Longitudinal dispersivity was determined within the laboratory experiments to $\alpha_l = 10^{-3}$ m, and transversal dispersivity was assumed to be $\alpha_t = 0.1 \times \alpha_l = 10^{-4}$ m. Following Sugio and Desai (1987), diffusion effects were neglected due to the primarily advection-dominated flow regime (Walther et al. 2012).

Although the domain becomes confined at $x \geq 0.25$ m, Goswami and Clement (2007) do not explicitly state a value for specific storativity. In this application, it is assumed that the response from the change of the right-side pressure head boundary condition happens relatively fast on this small scale and has only little impact on the saltwater wedge emerging from the left side.

### Results and discussion

Figure 2 depicts the comparison of the transient simulations between the experiment and the numerical models. In TS1 (Fig. 2a), the saltwater encroaches into the tank, increasing total intrusion length, whereas in TS2 (Fig. 2b), saline intrusion retreats again. Both simulation tools, SEAWAT and OPENGEOSYS, resemble the measurements quite well in terms of temporal development, shape of the saltwater wedge, and intrusion length.

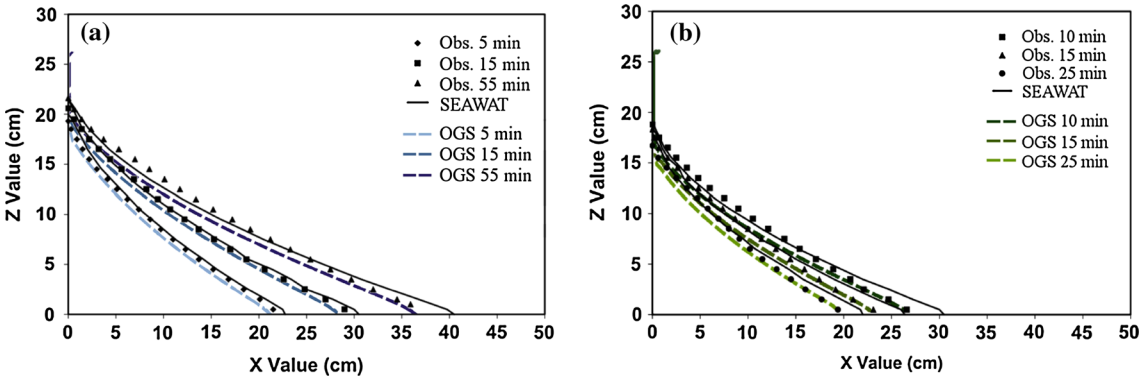


**Fig. 2** Concentration $c = 0.5$ isolines for Goswami–Clement's experimental observation data (*point symbols*), their SEAWAT simulation (*black lines*), and OGS results (*coloured lines*); after Goswami and Clement (2007) (altered). **a** Transient state TS1 (intrusion), **b** transient state TS2 (withdrawal)

Nevertheless, both numerical models also show deviations from the laboratory measurements. While SEAWAT overestimates intrusion length at the toe of the saltwater wedge, OGS generally yields a better prediction or slightly underestimates intrusion near to the lower boundary. Near the left-side saltwater boundary condition, SEAWAT results are in better compliance with measurements than the OGS outcome. This may be due to the circumstance that OGS does not feature a mass transport boundary condition, which is sometimes referred to as "constrain boundary condition". This particular boundary condition switches automatically between fresh or saltwater concentration depending on the flow direction, i.e., $c = c_s$ for flow into and $c = 0$ for flow out of the model domain.

As the modeling results show generally low deviations from the laboratory observations, we understand that OGS is able to represent the relevant density-driven flow processes.

## Regional scale model

With the successful benchmarking of OGS on experimental data, we furthermore applied the numerical tool on a real-world application. In the following, we shortly describe the study area of the regional scale model, and afterwards present and discuss results of the transient calibration and scenario simulation.

### Preceding work and model setup

#### *Model setup of real-world study area*

The near coastal groundwater study area consists of a three dimensional, heterogeneous aquifer with an extend of ca. $20 \times 30\,\text{km}^2$ and a maximum depth of 450 m in the centre of the domain ("Ma'awil trough"). Video 1 shows the hydrogeology of the model domain, with its twelve distinct material groups (1–12 as high to low permeability), and magnitude of flow velocity. Above a less permeable secondary aquifer, a thin and highly permeable primary aquifer can be seen at the coast, increasing in depth to the south until the Ma'awil trough. Aquifer regions with high flow velocities due to higher permeability are recognized by a more intense green saturation. The video is available in the OGS Youtube channel via the link http://youtu.be/_jx0wt6Q1Ow or as supplementary material.

Boundary conditions of the numerical model are upstream subsurface inflow from mountainous recharge regions, spatially distributed pumping abstraction near the coast, and given sea water level and salinity. More details on the characteristics of the study area and the setup of the hydrogeological and numerical model are described in (Walther et al. (2012), Figures 4, 6, 7 and Table 3).

A long-term stable steady state was assumed until 1974, whereas the transient simulation time includes the period 1974–2005, and the scenario simulation time in the years 2006–2506. For the transient simulation, a set of parameter combinations of hydraulic conductivity, mean annual subsurface inflow, and invariant pumping rates were inherited from the calibrated long-term stable steady state. The latter also provided initial values for groundwater level and saline intrusion.

#### *Transient calibration strategy*

Real-world data of the study area and aquifer parameters were scarce. In particular, distribution and values of hydraulic conductivity were only known at few locations (Macumber 1998), total pumping abstraction rate and development over time could only be estimated (Stanger 1987; Al-Shoukri 2008) and mean annual upstream inflow was given within a certain bandwidth (Gerner et al. 2012). From the uncertainty of the three afore-mentioned sensitive model parameters and boundary conditions, a multi-

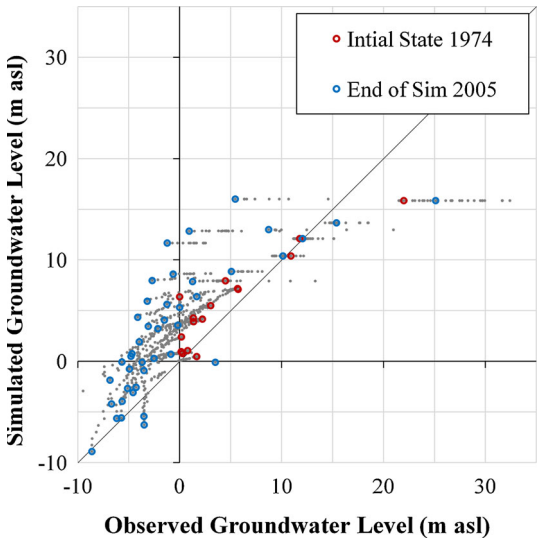


**Fig. 3** Scatter plot observed vs. simulated groundwater levels, *red dots* show initial state for transient simulation (1974), *blue dots* show final state (2005)

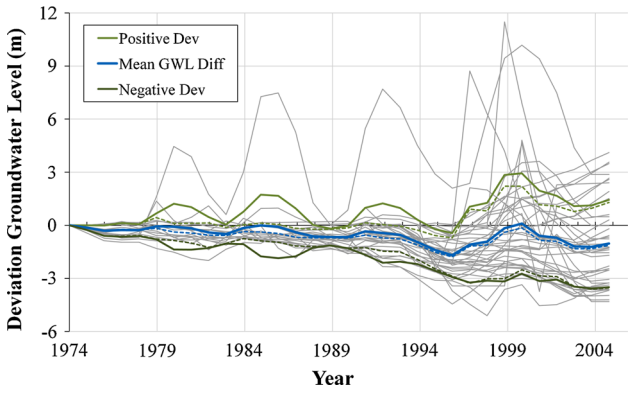


**Fig. 4** Difference of observed and simulated groundwater levels with subtracted initial difference (*grey lines*); *blue lines* mean value, *green lines* standard deviation from mean; *solid lines* with, *dashed lines* without oscillating observation well

dimensional matrix had to be calibrated. To find one reasonable parameter set, the following scheme was used to calibrate transient water levels and concentration.

Simulated groundwater levels were compared to 14 measurements available over the whole transient calibration period and additionally to several observation wells that were constructed during the transient period (up to 19 in year 2005). Saline intrusion was compared to published map data in terms of intrusion length and distribution along the coast (see also "Discussion"). Values of effective porosity for the twelve identified aquifer material groups were deducted and fixed following Macumber (1998) with a bandwidth of 0.05–0.17. Starting with the inherited steady-state parameter set, the parameter/boundary condition combination was changed to reduce deviations of the simulated from the observed values. Additionally, increase of pumping abstraction from pre-development phase in 1970s to year 2005 was used to calibrate the transient model.

## Transient calibration

### *Results*

*Groundwater table* Figure 3 shows a scatter plot for observed vs. simulated groundwater levels over the simulation time of 31 years. The initial state for 1974 (red dots in figure) could be calibrated with high correlation (correlation coefficient $R^2 = 0.83$). Within the calibration time (grey and blue dots), observation wells with low groundwater levels (i.e., near the coast) are met with only little deviation. However, simulated groundwater levels with higher values (i.e., further inland) generally show too high simulated values and no significant drawdown. Due to the deviations, the correlation coefficient reduced to $R^2 = 0.61$ for the year 2005.

For evaluating transient groundwater level behavior, we furthermore compare deviations of simulated from observed groundwater levels over time including subtraction of initial deviation of 1974 (Fig. 4). If the system behavior is resembled correctly in the model, the result would be a horizontal line covering the $x$ axis. The mean value of the difference (blue lines) shows little deviations from the optimal case, i.e., the general trend of simulated groundwater levels is in concordance with the observed ones. Deviations from the mean values (green lines) are small in the beginning, but increase to the end of the simulation period.

*Groundwater budget* Following Eq. 2, the groundwater budget was determined. Therefore, total groundwater fluxes flowing from the upstream inflow boundary condition to the coast and saline intrusion were calculated. Fluxes were evaluated as the net water flow through vertical planes which were placed with a displacement of 1 km parallel to the respective boundaries.

$$\Delta S = Q_{\text{rech}} + Q_{\text{intr}} - Q_{\text{abstr}} \tag{2}$$

where $\Delta S$ is storage change flux, $Q_{\text{rech}}$ is flux into the domain due to subsurface inflow of upstream recharge, $Q_{\text{intr}}$ is flux into the domain from marine seawater intrusion, and $Q_{\text{abstr}}$ is flux out of the domain due to pumping abstraction. The term $Q_{\text{intr}}$ evaluates the net flux through the budget surface near the coast, i.e., it becomes positive when the sum of all fluxes from seawater intrusion into the aquifer is greater than the fluxes from freshwater discharge into the sea. The same remains true for the opposite case.

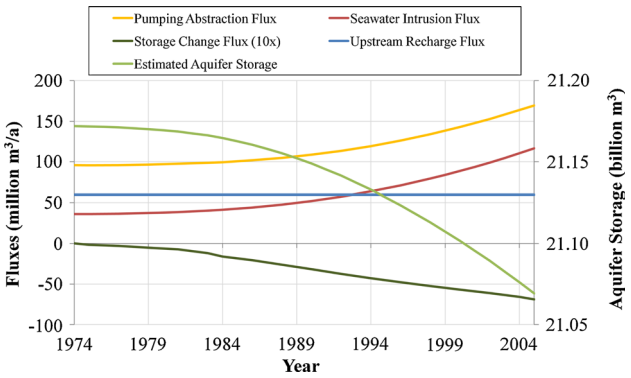


**Fig. 5** Water fluxes and estimated aquifer storage in model area within transient simulation period; NB: storage change flux plotted with 10 times exaggeration

Figure 5 plots the development in time of groundwater fluxes, abstraction rates, as well as aquifer storage for transient simulation time. Inflow from upstream recharge remains constant over time. As pumping rates increase, aquifer storage decreases, and saltwater intrusion raises. Although total estimated storage volume is very large, relatively small changes in aquifer storage unbalance the groundwater regime leading to the apparent problems (groundwater drawdown, saline intrusion etc.). Marine saltwater intrusion in 2005 was estimated as $118 \times 10^6\,m^3/a$, and total abstraction rate as $183 \times 10^6\,m^3/a$ which is in good accordance with published estimations (Al-Shoukri 2008; Ministry of Agriculture and Fisheries 2012).

*Salinity* Simulation output of marine intrusion (Fig. 6a, b) shows results for intrusion length and spatial variability along the coast similar to reported measurements (Ministry of Agriculture and Fisheries 2012). Mean intrusion length and the general trend of saltwater intrusion increase from 2–4 km in 1975 to 5–7 km in 2005. Groundwater flow paths are indicated by stream tracers, originate in the southern mountainous areas and, in 1974, still partly reach the sea. As freshwater discharges into the sea, the intrusion interface is still retained near the coast. In 2005 (Fig. 6b), all recharge plumes are completely captured by pumping activities. High abstraction rates lead to immense drawdown and accordingly excessive saltwater intrusion of up to 3 km. The variability of the marine intrusion along the coast is depending on the local hydrogeology, the subsequent spatially highly variable flow regime (Fig. 7), and locally distributed pumping activities.

Video 2 shows the salinity distribution and flow paths through stream tracers originating in the southern and near coastal model domain exemplary for 1985. The effect of the heterogeneous permeability distribution can be recognized through the interlaced flow paths of the stream tracers that eventually merge into convection cells at the salt–freshwater interface, which are typical for density-driven flow. The video is available via the OGS Youtube channel at http://youtu.be/-xBQJ9WWPJY or as supplementary material.

## *Discussion*

A general reason for the deviations in groundwater level might be explained by the uncertainty of the boundary condition for pumping activity. As no detailed information on abstraction rates is available, this boundary condition was derived from over 5,000 known locations of pumps using an areal density filter assuming constant abstraction for every single pump (compare Walther et al. 2012; Figure 7). The resulting discrete polygons for applying the abstraction boundary condition exclude areas with low areal density of pumps, as it is the case in regions far from the coast. When these pump units are stronger, single pumps might have a significant influence on the groundwater table. However, more detailed information about individual abstraction rates is not known.

Larger divergences (higher standard deviations) in the end of simulation time might be due to upcoming industrialization of agriculture, when dug wells with generally similar abstraction rates were partially replaced by drilled boreholes and pumps with higher variation of abstraction potentials. Again, this information is not explicitly available.

Periodic oscillations of the groundwater levels, as observed by one of the monitoring wells that are situated near to the mountainous recharge region, are probably due to medium-term precipitation cycles. Neglecting this specific observation yields a much smaller standard deviation from the mean value especially for the first half of the simulation time (see dashed lines in Fig. 4). Currently, such an oscillating boundary could not be included as underlying data, i.e., frequency and amplitude, are not available. Investigations using a simplified 2D model with a fluctuating inflow boundary condition could show that the model is able to reproduce the observed behavior in principle, i.e., oscillating groundwater levels near the recharge area, which are dampened in closer distance to the sea boundary condition.

Deviations of marine intrusion may be due to several reasons: structure and parameters of the hydrogeology, as well as abstraction rates of groundwater pumps are not exactly known; spatial and temporal limited recharge events in wadi channels, which are not included in the simulation, might influence short-term groundwater levels and salinity; and finally, published maps show doubtful

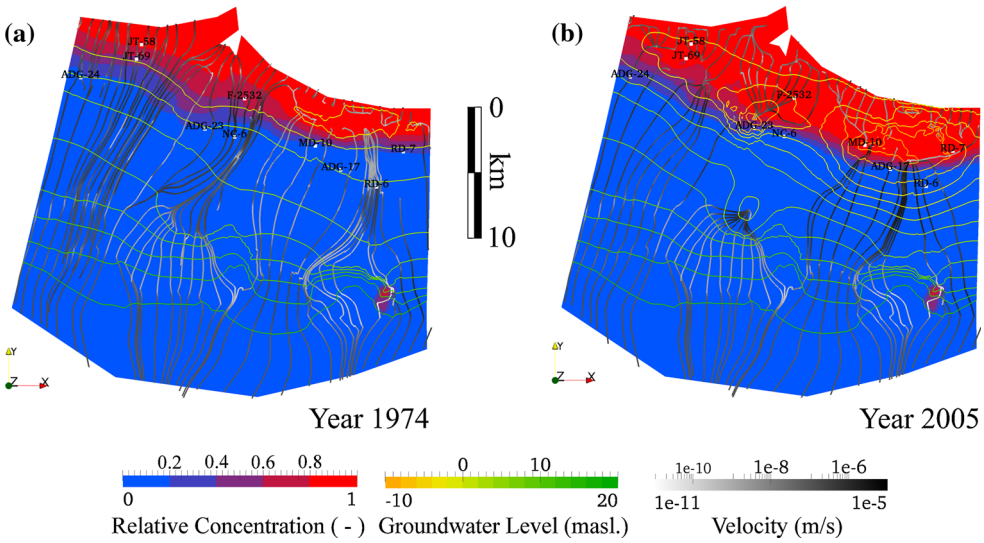


**Fig. 6** Salinity (at 10 m below groundwater level), groundwater levels (isolines) and stream tracer for initial and final state of transient simulation (1974 and 2005), after Walther et al. (2013)

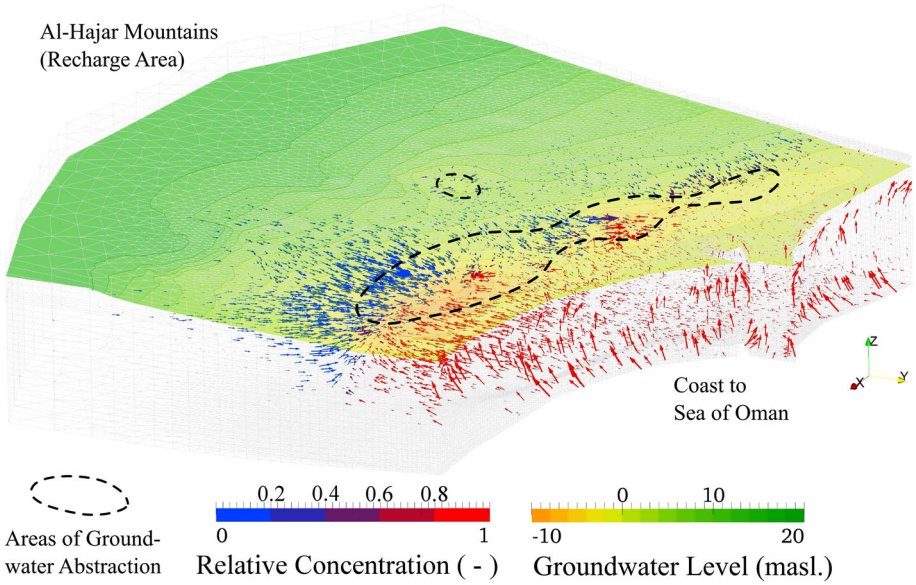


**Fig. 7** Groundwater model domain, final state of transient simulation (year 2005); groundwater levels, scaled velocity vectors with relative concentration; *dashed lines* symbolize major areas of groundwater abstraction, after Walther et al. (2013)

salinization development, e.g., reduction of salinity in a "sabkha" (a salt desert) at the northern coastal stretch between 1995–2010 [compare Ministry of Agriculture and Fisheries (2012)].

## Remediation scenario simulation

To assess the remediation potential of the aquifer, a "best-case" scenario simulation was carried out with the assumption that all pumping activities were ceased after year 2005. Additionally, we assume that the withdrawal of the saltwater will not involve any retention processes (e.g., reversable adsorption, double porosity continuum). The scenario simulation time was 500 years.

### *Medium-term projection*

Figure 8 presents groundwater levels and flow paths (via stream tracers) at the scenario time 2105, i.e., 100 years after pump stop. Comparing the results from the year 2005, where abstraction was the highest (Fig. 6b), even after 100 years of no pumping activity (Fig. 8), mountainous recharge plumes only partly reach the sea again and slowly refill the aquifer storage. Also, groundwater levels and salinity did not return to their former values in the 1970s.

In Fig. 9, salinity is plotted against groundwater drawdown for 1974 until 2070; each arrow symbolizes 1 year. General behavior shows increasing drawdown (due to pumping) and thus growing salinity. When pumping stops

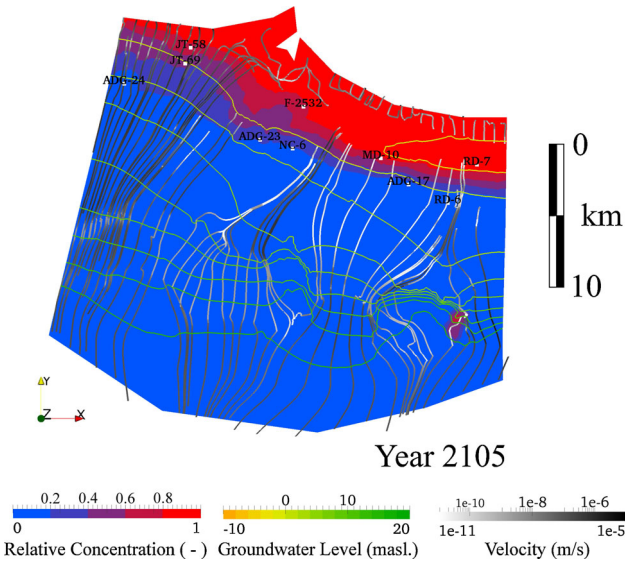


**Fig. 8** Salinity (at 10 m below groundwater level), groundwater levels (isolines) and stream tracer for scenario time 2105; after Walther et al. (2013)

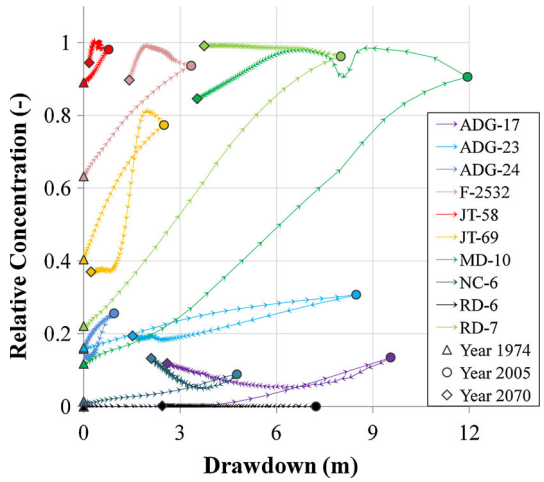


**Fig. 9** Salinity vs. drawdown over time, scenario simulation for ca 100 years (1974–2070), increase of pumping starting 1974, stop pumping after year 2005; each *arrow* symbolizes 1 year; after Walther et al. (2013)

(2005), drawdown slowly recovers, but salinity mostly still raises revealing a hysteresis: although there is no groundwater abstraction after 2005, the hydraulic gradient still points from the sea into the pumps' direction. Hence, saline concentrations continue to increase. High salinization is possible even with only small drawdown (e.g., 'JT-69', location shown in Fig. 8). Maximum drawdown, however, is up to 12 m within 30 years of pumping activity. Recovery times of groundwater levels are supposedly

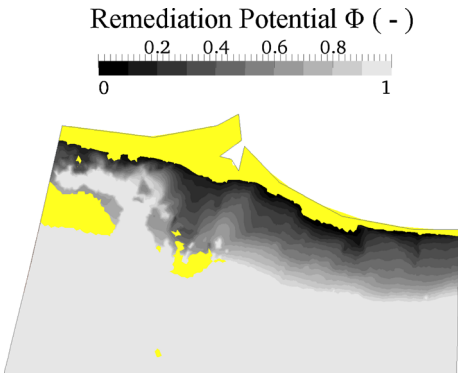


**Fig. 10** Salinity remediation potential of coastal area 10 m below groundwater level (0 = low potential, 1 = high potential) based on the salinity half-life after pump stop; yellow areas do not reach half initial concentration within 500 years, after Walther et al. (2013)

>100 a and even longer for salinity. Even when drawdowns approach zero, i.e., groundwater levels same as in initial state 1974, salinity is mostly higher than in the beginning of simulation.

*Long-term remediation potential*

To assess long-term remediation capabilities, Fig. 10 shows heterogeneous patterns of $\Phi$ along the coast (see Eq. (1)). The isolines of $\Phi$ are relatively parallel to the coast line in the eastern area. Remediation potential appears to be relatively high as soon as abstraction is reduced. This may result from the aquifer's properties and high yield, and the corresponding preferred area of high abstraction activity. In the western area, the remediation potential is relatively high (due to a high mobility in porous media). The remediation potential drops where mobility is low. Low remediation potentials in the south of the coastal bay, where permeability is very low, might pose a reason for the development of the sabkha. Yellow color symbolizes areas where the remediation potential does not fall below $0.5 \cdot c_{rel}$ within 500 years of simulation. Such areas near the coast are probably showing the undisturbed situation of marine salinity intrusion (i.e., no groundwater abstraction). Areas further inland are due to low permeable hydrogeology.

Groundwater budgets for the scenario simulation time are plotted in Fig. 11. A complete pumping stop results in slowly replenishing aquifer storage, as both, marine saltwater intrusion and upstream groundwater recharge aid to recover decreased groundwater levels. Eventually, the marine intrusion flux becomes smaller than the recharge flux and even changes direction, so that more freshwater flows out of the domain leaking into the ocean than seawater flows into the aquifer (ca. year 2220). The scenario

water budgets indicate once more that the reversal of the current saltwater intrusion to a naturally balanced regime needs a long-term remediation approach.

### Visualization in virtual reality

Nowadays, numerical models more and more increase in degree of detail and resolution. As simulation results simultaneously gain additional levels of complexity, a profound interpretation of the modeling outcome requires potent visualization tools Helbig et al. (2014).

Besides the presented 2D figures and videos, and similar to Sun et al. (2012), we therefore utilized a virtual reality centre with a high-resolution video wall using stereoscopic projection and an optical tracking system (Fig. 12, VISLAB 2013). The interactive, three-dimensional visualization tool, provides an immersive environment, offering the possibility to acquire inside knowledge on the model's behavior. Rink et al. (2014) give a detailed description on further possibilities and applications of the virtual reality centre. Especially for the presented case study, where the numerical model included a heterogeneous parameter distribution in a three-dimensional domain, a virtual reality proofed to be useful during model setup (hydrogeological parameter distribution) and later for detailed investigations and proper interpretations of simulation results (compare e.g., supplementary materials Video 1 and 2, "Regional Scale Model"). Furthermore, this exceptional visualization type also helped transporting scientific findings to Omani representatives during their visit, supporting their decision making process.

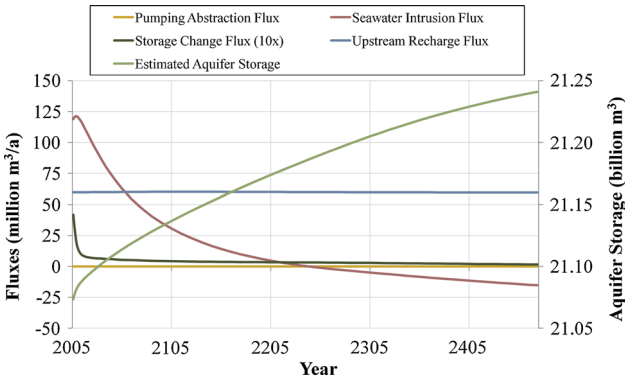


**Fig. 11** Water fluxes and estimated aquifer storage in model area within scenario simulation period; NB: storage change flux plotted with 10 times exaggeration

## Conclusions and outlook

When real-world data are scarce and, if available, additionally show suspicious measurement values, fitting of observations to simulation results is cumbersome and difficult to carry out. Yet, after setting up and parameterizing a numerical model in all conscience, modeling results can aid in an overall fundamental assessment of the target area. An examination of the general trend of the results can give

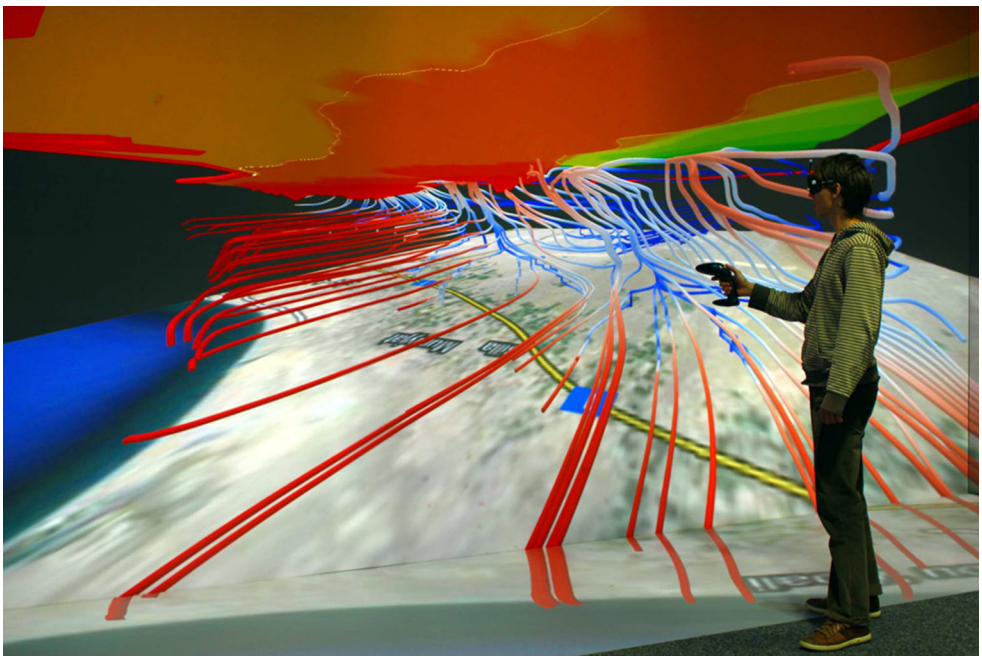

**Fig. 12** Three-dimensional visualization of simulation data in the TESSIN-VISLab at the UFZ Leipzig

information on the success of the calibration and furthermore help to identify possible measurement activities. This, in turn, may increase model robustness and prediction quality or delineate future system behavior to support decision makers.

In the situation at hand, the modeling results are not in perfect agreement with the measurements. Yet, simulated values of the groundwater level are similar to measurements showing a comparable general behavior. Calculated water balances reveal plausible ranges of the individual components. Marine saltwater intrusion shows a comparable extent, areal heterogeneity along the coast, as well as development in time. Although a "pump stop" might not be a practicable action, the best-case scenario simulation reveals a temporal dimension for remediation and overall salinization risk in the study area. Scientific visualization helped to evaluate the hydrogeological setup and draw conclusions from the modeling output.

Although the data base was relatively weak compared to the typical requirements for this type of modeling including hydrogeological heterogeneities, the numerical model still proved to be a useful tool. Scenario results stress the vulnerability of the local aquifer system with its sensitive balance of the fresh–saltwater interface. In particular, the outcome underlines the necessity of an immediate action plan to prevent further saline intrusion or even total loss of the usability of the aquifer's groundwater resources.

**Acknowledgments** The authors acknowledge the funding by the German Federal Ministry of Education and Research (BMBF Number: FKZ 02WM1166, IWAS), and by the Ministry of Science, Research and Arts of Baden-Württemberg (AZ Zu 33-721.3-2). The authors are grateful for the sincere cooperation of the Omani colleagues from the Ministry of Regional Municipalities and Water Resources, Muscat. The authors would like to thank the anonymous reviewers for their time and effort to read and comment on the manuscript increasing impact and quality of the publication.

## References

Abd-Elhamid H, Javadi A (2011) A density-dependant finite element model for analysis of saltwater intrusion in coastal aquifers. J Hydrol 401(3–4):259–271. doi:10.1016/j.jhydrol.2011.02.028. URL http://linkinghub.elsevier.com/retrieve/pii/S0022169411001430

Al-Shoukri SSM (2008) Mathematical Modeling of Groundwater Flow in Wadi Ma'awil Catchment, Barka in Sultanate of Oman. Master's thesis, Arabian Gulf University, Bahrain

Bureau de Recherches Géologiques et Minières (BRGM) (1992) Study of A New Organization of Irrigation in Barka-Rumais Area: Data Analysis and Modelling Report. Tech. Rep. 33, BRGM L'ENTREPRISE AU SERVICE DE LA TERRE

Gerner A, Schütze N, Schmitz GH (2012) Portrayal of fuzzy recharge areas for water balance modelling - a case study in northern Oman. Adv Geosci 31:1–7. doi:10.5194/adgeo-31-1-2012. http://www.adv-geosci.net/31/1/2012/

Giambastiani B, Antonellini M (2007) Saltwater intrusion in the unconfined coastal aquifer of Ravenna (Italy): a numerical model. J Hydrol 340(1–2):91–104. doi:10.16/j.jhydrol.2007.04.001. http://www.sciencedirect.com/science/article/pii/S0022169407002119

Goswami RR, Clement TP (2007) Laboratory-scale investigation of saltwater intrusion dynamics. Water Resour Res 43(4):1–11. doi:10.1029/2006WR005151

Grundmann J, Schütze N, Schmitz G, Al-Shaqsi S (2012) Towards an integrated arid zone water management using simulation-based optimisation. Environ Earth Sci, pp 1381–1394. doi:10.1007/s12665-011-1253-z. http://www.springerlink.com/index/U4767301353M2755.pdf

Helbig C, Bauer HS, Rink K, Wulfmeyer V, Frank M, Kolditz O (2014) Concept and workflow for 3D visualization of atmospheric data in a virtual reality environment for analytical approaches. Environ Earth Sci (this issue). doi:10.1007/s12665-014-3136-6

Henderson A (2007) ParaView Guide, A Parallel Visualization Application. Kitware Inc., http://www.paraview.org

Henry HR (1960) Salt intrusion into coastal aquifers. PhD thesis, Columbia University, New York, USA

Kalbacher T, Delfs JO, Shao H, Wang W, Walther M, Samaniego L, Schneider C, Kumar R, Musolff A, Centler F, Sun F, Hildebrandt A, Liedl R, Borchardt D, Krebs P, Kolditz O (2011) The IWAS-ToolBox: Software coupling for an integrated water resources management. Environ Earth Sci 65(5):1367–1380. doi:10.1007/s12665-011-1270-y

Kalbus E, Kalbacher T, Kolditz O, Krüger E, Seegert J, Röstel G, Teutsch G, Borchardt D, Krebs P (2011) Integrated Water Resources Management under different hydrological, climatic and socio-economic conditions. Environ Earth Sci 65(5):1363–1366. doi:10.1007/s12665-011-1330-3

Kolditz O, Ratke R, Diersch HJG, Zielke W (1998) Coupled groundwater flow and transport: 1. Verification of variable density flow and transport models. Adv Water Resour 21(1):27–46. doi:10.1016/S0309-1708(96)00034-6. http://www.sciencedirect.com/science/article/pii/S0309170896000346

Kolditz O, Bauer S, Bilke L, Böttcher N, Delfs JO, Fischer T, Görke UJ, Kalbacher T, Kosakowski G, McDermott CI, Park CH, Radu F, Rink K, Shao HB, Sun F, Sun YY, Singh aK, Taron J, Walther M, Wang W, Watanabe N, Wu Y, Xie M, Xu W, Zehner B (2012a) OpenGeoSys: an open-source initiative for numerical simulation of thermo-hydro-mechanical/chemical (THM/C) processes in porous media. Environ Earth Sci 67(2):589–599. doi:10.1007/s12665-012-1546-x

Kolditz O, Görke UJ, Shao H, Wang W (2012b) Thermo-hydro-mechanical-chemical processes in porous media: benchmarks and examples. In: Lecture notes in computational science and engineering. Springer, Berlin

Krueger EH, Teutsch G (2013) International viewpoint and news. Environ Earth Sci. doi:10.1007/s12665-013-2280-8

Langevin CD, Guo W (2006) MODFLOW/MT3DMS-based simulation of variable-density ground water flow and transport. Ground Water 44(3):339–351. doi:10.1111/j.1745-6584.2005.00156.x

Macumber PG (1998) The Cable Tool Program and Groundwater Flow in the Eastern Batinah Alluvial Aquifer. Ministry of Water Resources, Muscat, Oman

Ministry of Agriculture and Fisheries (2012) OMAN SALINITY STRATEGY (OSS) Oman Salinity Strategy. Tech. rep., Ministry Of Agriculture And Fisheries (MAF), Sultanate Of Oman International Center For Biosaline Agriculture (ICBA) Dubai, UAE.

Narayan Ka, Schleeberger C, Bristow KL (2007) Modelling seawater intrusion in the Burdekin Delta Irrigation Area, North Queensland, Australia. Agric Water Manag 89(3):217–228, doi:10.1016/j.agwat.2007.01.008, http://linkinghub.elsevier.com/retrieve/pii/S0378377407000327

Neuman SP (1974) Effect of partial penetration on flow in unconfined aquifers considering delayed gravity response. Water Resour Res 10(2):303–312. doi:10.1029/WR010i002p00303

Park CH (2004) Saltwater intrusion in coastal aquifers. PhD thesis, Georgia Institute of Technology

Park CH, Aral M (2008) Saltwater intrusion hydrodynamics in a tidal aquifer. J Hydrol Eng 13(September):863

Rink K, Bilke L, Kolditz O (2014) Visualisation strategies for environmental modelling data. Environ Earth Sci. doi:10.1007/s12665-013-2970-2

Schroeder W, Martin K, Lorensen B (2006) The Visualization Toolkit: An Object-oriented Approach to 3D Graphics. Kitware, http://books.google.de/books?id=rx4vPwAACAAJ

Schütze N, Kloss S, Lennartz F, Bakri AA (2012) Optimal planning and operation of irrigation systems under water resource constraints in Oman considering climatic uncertainty. Environ Earth Sci, pp 1511–1521, doi:10.1007/s12665-011-1135-4. http://www.springerlink.com/index/RRW27U324587K637.pdf

Siebert S, Burke J, Faures JM, Frenken K, Hoogeveen J, Döll P, Portmann FT (2010) Groundwater use for irrigation a global inventory. Hydrol Earth Syst Sci 14(10):1863–1880, doi:10.5194/hess-14-1863-2010. http://www.hydrol-earth-syst-sci.net/14/1863/2010/

Stanger G (1987) The Hydrogeology of the Oman Mountains. PhD thesis

Sugio S, Desai CS (1987) Residual flow procedure for sea water intrusion in unconfined aquifers. Int J Numer Methods Eng 24(8):1439–1450. doi:10.1002/nme.1620240803

Sun F, Shao H, Wang W, Watanabe N, Bilke L, Yang Z, Huang Z, Kolditz O (2012) Groundwater deterioration in Nankoua suburban area of Beijing: data assessment and remediation scenarios. Environ Earth Sci 67(6):1573–1586. doi:10.1007/s12665-012-1600-8

Theis C (1935) The relation between the lowering of the piezometric surface and the rate and duration of discharge of a well using groundwater storage. Trans Am Geophys Union 16:513–514

VISLAB (2013) Visualization Center - Helmholtz-Zentrum für Umweltforschung UFZ. http://www.ufz.de/index.php?en=14171

Walther M, Delfs JO, Grundmann J, Kolditz O, Liedl R (2012) Saltwater intrusion modeling: verification and application to an agricultural coastal arid region in Oman. J Comput Appl Math 236(18):4798–4809. doi:10.1016/j.cam.2012.02.008

Walther M, Bilke L, Delfs JO, Graf T, Grundmann J, Kolditz O, Liedl R (2013) Visualizing Saline Intrusion in a Three-Dimensional, Heterogeneous. Coastal Aquifer. In: Workshop on Visualisation in Environmental Sciences (EnvirVis), Leipzig

Werner AD, Bakker M, Post VE, Vandenbohede A, Lu C, Ataie-Ashtiani B, Simmons CT, Barry D (2012) Seawater intrusion processes, investigation and management: recent advances and future challenges. Adv Water Resour doi:10.1016/j.advwatres.2012.03.004, http://linkinghub.elsevier.com/retrieve/pii/S030917081200053X